LANGLEY GRANT
IN-32-CR
150135
P-29

SCATTERING PATTERNS OF DIHEDRAL CORNER REFLECTORS WITH IMPEDANCE SURFACE IMPEDANCES

Semiannual Report

Constantine A. Balanis, Timothy Griesser, and Kefeng Liu

February 1 - July 31, 1988

Department of Electrical and Computer Engineering
Arizona State University
Tempe, AZ 85287

(NASA-CR-183078) SCATTERING PATTERNS OF DIHEDRAL CORNER REFLECTORS WITH IMPEDANCE SURFACE IMPEDANCES Semiannual Report, 1 Feb. - 31 Jul. 1988 (Arizona State Univ.) 29 p CSCL 20N G3/32

N88-26545

Unclas
0150135

Grant No. NAG-1-562
National Aeronautics and Space Administration
Langley Research Center
Hampton, VA 23665

ABSTRACT

The radar cross section patterns of lossy dihedral corner reflectors are calculated using a uniform geometrical theory of diffraction for impedance surfaces. All terms of up to third order reflections and diffractions are considered for patterns in the principle plane. The surface waves are included whenever they exist for reactive surface impedances. The dihedral corner reflectors examined have right, obtuse, and acute interior angles, and patterns over the entire 360° azimuthal plane are calculated. The surface impedances can be different on the four faces of the dihedral corner reflector; however the surface impedance must be uniform over each face. Computed cross sections are compared with a moment method technique for a dielectric/ferrite absorber coating on a metallic corner reflector. The analysis of the dihedral corner reflector is important because it demonstrates many of the important scattering contributors of complex targets including both interior and exterior wedge diffraction, half-plane diffraction, and dominant multiple reflections and diffractions.

I. INTRODUCTION

For many years, engineers have investigated how the shape and material properties of complex objects affect their backscattering patterns. The interest in this area is primarily aimed toward using appropriate shaping along with lossy or coated materials to reduce the radar cross section of complex targets, such as aircraft. A large majority of the published research in this area concerns mainly the perfectly conducting surfaces for which extensive analytical techniques exist. Only recently has published work been available on complex targets constructed of lossy or composite materials.

In this paper, backscattering from one of the most fundamental complex targets, the dihedral corner reflector, is considered using the recently available uniform geometrical theory of diffraction (UTD) for interior impedance wedges [1]. Uniform asymptotic theories for exterior impedance wedges have also been considered in [2] and [3]. The dihedral corner reflector is formed by attaching two rectangular plates along a common edge and separating the plates by a specified interior angle. The impedance surface boundary condition is assumed, and the plates are permitted to have different impedances on the four faces although the impedances must be uniform over each face. The impedance surface boundary condition is one of the most common approximations to the exact boundary conditions on lossy surfaces, and its validity has been discussed by several authors [4]-[6]. It is a useful approximate boundary condition because it allows mathematically tractable results while giving accurate answers.

The dihedral corner reflector with impedance surfaces demonstrates many of the scattering mechanisms which exist on more complex lossy structures. It includes three types of diffracting wedges; the half plane, the exterior wedge and the interior wedge. In addition, the dihedral corner reflector has very dominant higher order reflections and diffractions, and it is these higher order terms which are often the important scattering mechanisms of complex structures. Of particular interest is the 90° dihedral corner reflector because 90° corners often exist on many complex targets. This corner reflector has a very strong double reflection which dominates the backscatter pattern in the forward region. For the impedance surface case considered, the lossy reflection reduces the magnitude of the backscattered field, and, in a double reflection, that loss is encountered once at each reflection. The dihedral corner reflector then is a very important target for studying the effectiveness of surface coatings and composite materials as well as for examining the properties of various interior and exterior angles and plate sizes.

The perfectly conducting dihedral corner reflector has been examined previously using both physical and geometrical theories. Knott [7] used a physical optics analysis for single and double reflections to determine the backscattering reduction achieved by varying the interior angle of the corner reflector. Anderson [8] added higher order reflections to this physical optics method and further investigated the effects of the dihedral angle. Griesser and Balanis [9] used physical optics and the physical theory of diffraction to examine the corner reflector in the full azimuthal plane and to demonstrate tradeoffs in

accuracy and complexity of physical optics and physical diffraction techniques. Michaeli [10] presented a refined analysis of the scattering from a 90° dihedral corner reflector illuminated near grazing incidence. The dihedral corner reflector was first studied using the uniform theory of diffraction (UTD) by Yu and Huang [11] in the forward region. Griesser and Balanis [12] improved the UTD model by adding all possible multiple reflection and diffraction terms of up to third order for the entire azimuthal plane. The dihedral corner reflector for the lossy surface impedance case has recently been studied by Corona, Ferrara and Gennarelli [13]. In [13], only backscattering from a 90° dihedral corner reflector for ±45° on each side of the forward direction was considered using physical optics refined by a UTD technique. The UTD was added to the geometrical optics field for the double reflection only. The method cannot be extended to corner reflectors of other interior angles because no physical diffraction coefficient is available for the interior wedge of arbitrary angle.

In this work, the lossy dihedral corner reflector is examined using geometrical optics refined by the uniform geometrical theory of diffraction for impedance surfaces. An imposed edge is added near normal incidence to the reflecting plates in the forward region to achieve continuity near the major lobes [12]. Different surface impedances are allowed on each of the four dihedral corner reflector faces, and the cross section patterns are the same as for the perfectly conducting case [12] when the surface impedance approaches zero. The method is based upon the newly derived diffraction coefficients for the interior impedance wedge [1] which have the same form as the perfectly

conducting UTD with suitable Maliuzhinet's functions as multiplying factors. Also, using [1], the surface waves are readily added to the diffraction terms. Both vertical and horizontal polarizations are considered for backscatter patterns of dihedral corner reflectors computed in the principle plane. The entire 360° azimuthal plane is investigated using this technique to distinguish the effects of both interior and exterior reflections and diffractions. Surface waves are included in the analysis. In general, surface waves exist only for certain reactive surface impedances whose range of values is a function of polarization.

II. ANALYTICAL METHOD

The dihedral corner reflector with lossy surfaces is illustrated in Fig. 1. It is formed by connecting two flat rectangular plates at a common edge, and the plate sizes and orientations are specified in the figure. The radar cross section is computed in the principle azimuthal plane; that is, the x-y plane, in the angular direction ϕ measured from the x axis. Following common practice, the range of observation R should be larger than $2D^2/\lambda$ where D is the largest dimension of the corner reflector and where λ is the free space wavelength. The vertical and horizontal polarizations are considered. For the vertical polarization the electric field vector is parallel to the z-axis while for the horizontal polarization it is perpendicular to the z-axis. An $e^{j\omega t}$ time convention is assumed and suppressed. The complexity of the backscatter analysis is reduced by considering the dihedral corner

reflector to be a short segment of a longer two-dimensional object extending toward infinity along the z-axis [12].

It is first desirable to tabulate the possible backscattering terms necessary for computing the radar cross section of the dihedral corner reflector in the azimuthal plane. As shown in Fig. 1, there are four diffracting edges and four reflecting surfaces in the dihedral corner reflector geometry. The diffracting edges are numbered 1, 3, 5, and 7 while the reflecting surfaces are numbered 2, 4, 6, and 8. The normalized surface impedances on each face are defined as η_2, η_4, η_6 and η_8. Each surface impedance is normalized to the free space value, and the impedances are required to be uniform over each individual face. The η=0 case corresponds to the perfect electric conductor while η=∞ represents a (non-physical) perfect magnetic conductor. These eight reflecting and diffracting elements yield eight first-order scattering terms.

It is obvious that a first-order analysis is insufficient for the complex geometry of the dihedral corner reflector. It is well known that the dominant scattering terms are the higher-order reflections and diffractions; hence it is necessary to add higher order terms. In total, there are sixteen second-order mechanisms and forty third-order mechanisms to consider. For smaller interior dihedral corner reflectors it is necessary to progress even to fourth-order terms. To lend some organization to the analysis, a special naming convention is used to identify particular scattering components; each component will be preceded by a capital letter C, and each will include digits corresponding to the order of the associated reflections and

diffractions, as defined by the numbering convention of Fig. 1. For example, C142 corresponds to a ray which is initially incident on and diffracted by edge 1, then is reflected by surface 4, and finally reflected by surface 2 toward the observation point. C15 is a ray which is initially incident upon and diffracted by edge 1, and then diffracted by edge 5 back to the observation point. The complete listing of all necessary terms is as follows:

First-order terms

C1 C2 C3 C4 C5 C6 C7 C8

Second-order terms

C13 C14 C15 C17 C24 C25 C31 C35

C41 C42 C51 C52 C53 C57 C71 C75

Third-order terms

C131	C135	C141	C142	C151	C152	C153	C157
C171	C175	C241	C242	C251	C252	C253	C313
C314	C315	C351	C352	C353	C413	C414	C415
C424	C425	C513	C514	C515	C517	C524	C525
C531	C535	C571	C575	C715	C717	C751	C757

In addition the imposed edges of [12] are included at the geometrical optics shadow boundaries of surfaces 2 and 4. The lists could be reduced if some symmetry is introduced to the problem; that is, if both plates are of identical sizes and impedances. Each term exists only over a finite angular range which is determined by the geometry of the problem [12], [14]. In addition, for a particular reflector at a given orientation some terms will be very dominant while others may be negligible. However in some other direction or for a different interior

angle, the negligible terms may become the dominant terms, hence it is best to include as many terms as practical. In fact for small interior angles it may be necessary to progress to fourth order terms.

Each of the backscattering terms for the two-dimensional dihedral corner reflector can be written as a product of the incident field and the appropriate reflection coefficients, diffraction coefficients, spreading factors and phase factors. To simplify the geometrical considerations, the reflections of rays are accounted for by utilizing the method of images. All images of the source and the diffracting edges are located through the reflecting surfaces. In this manner, the problem reduces to terms which involve only the rays from the source or its image diffracting off edges or their images. For a particular component, the reflections, if any, are numbered 1 through p, and the diffractions, if any, are numbered 1 through q. Each of the backscattered terms can then be written as

$$U^s=\left[U_0\ \frac{e^{-jk\rho_0}}{\sqrt{\rho_0}}\right]\left[\prod_{j=1}^{p}\Gamma_j(\varphi_j,\theta_j)\right]\left[\prod_{i=1}^{q}D(\phi_i',\phi_i,\frac{\rho_{i-1}\rho_i}{\rho_{i-1}+\rho_i},n_i,\theta_0^i,\theta_n^i)\ \frac{e^{-jk\rho_i}}{\sqrt{\rho_i}}\right] \tag{1}$$

The first term corresponds to the incident field, the second term corresponds to the product of the reflection coefficients, and the third term corresponds to the product of diffraction coefficients, spreading factors and phase factors. For vertical polarization $U^s=E^s$ and $U_0=E_0$ while for horizontal polarization $U^s=H^s$ and $U_0=H_0$. The distance from the source (or its image) to the first diffracting edge is ρ_0. The distance ρ_i is the distance from the i^{th} diffracting edge to the next

diffracting edge or the observation point. Alternatively, the distance ρ_{i-1} is the distance from the i^{th} diffracting edge to the previous diffracting edge or the source point. The angles ϕ_i' and ϕ_i are measured from the 0 face of the i^{th} diffracting edge in the direction of incidence and diffraction, respectively. The edge wedge parameter n_i and the impedance angles θ_0^i and θ_n^i similarly correspond to the i^{th} wedge. The lossy wedge diffraction coefficient $D(\phi',\phi,\rho,n,\theta_0,\theta_n)$ is defined in [1]. This recently derived coefficient is valid for both interior and exterior impedance wedges, and it is similar in form to the perfectly conducting case with suitable multiplying factors based on the Maliuzhinets function. It provides the proper discontinuities to compensate for discontinuities at shadow boundaries for all lossy multiple reflections of any order for any surface impedance. For the vertical polarization, $\theta_0=\sin^{-1} 1/\eta_0$ and $\theta_n=\sin^{-1} 1/\eta_n$, and for the horizontal polarization, $\theta_0=\sin^{-1}\eta_0$ and $\theta_n=\sin^{-1}\eta_n$. The angles θ_0 and θ_n represent the Brewster angles for which there is no reflection from the corresponding face for the given polarization. The reflection coefficient $\Gamma_j(\varphi_j,\theta_j)$ corresponds to reflection from the j^{th} surface and is a function of both the grazing angle of incidence φ_j and the Brewster angle θ_j. For the lossy surface reflection the reflection coefficient is given by

$$\Gamma_j(\varphi_j,\theta_j) = \frac{\sin\varphi_j - \sin\theta_j}{\sin\varphi_j + \sin\theta_j} \qquad (2)$$

To include the surface wave terms in the cross section analysis, it is necessary to modify the third term in (1) which includes the product of diffraction coefficients, spreading factors and phase factors. For plane wave incidence, the surface wave term and the associated surface wave transition function have been given in [1] as $U_{sw}(\phi',\phi,\rho,n,\theta_0,\theta_n)$ + $U_{SWTR}(\phi',\phi,\rho,n,\theta_0,\theta_n)$ with associated bounds on their regions of existence being implied. For a given polarization, each term exists only for a certain range of surface impedances. Unfortunately, there is no solution to the impedance wedge problem for cylindrical wave incidence from which surface waves can be derived. Hence it is only possible to utilize the surface wave terms derived for plane wave incidence as approximations to the cylindrical wave case. For the first diffracting edge this is a justifiable approximation because the source is at a far distance. For multiply diffracted terms it may be a less accurate approximation. To include the surface wave and its associated transition field, (1) becomes

$$U^s = \left[U_0 \frac{e^{-jk\rho_0}}{\sqrt{\rho_0}}\right]\left[\prod_{j=1}^{p} \Gamma_j(\varphi_j,\theta_j)\right]$$

$$\cdot \left[\prod_{i=1}^{q-1} D(\phi_i',\phi_i, \frac{\rho_{i-1}\rho_i}{\rho_{i-1}+\rho_i}, n_i,\theta_0^i,\theta_n^i) \frac{e^{-jk\rho_i}}{\sqrt{\rho_i}}\right.$$

$$\left. + U_{sw}(\phi_i',\phi_i,\rho_i,n_i,\theta_0^i,\theta_n^i) + U_{SWTR}(\phi_i',\phi_i,\rho_i,n_i,\theta_0^i,\theta_n^i)\right]$$

$$\cdot D(\phi_q',\phi_q, \frac{\rho_{q-1}\rho_q}{\rho_{q-1}+\rho_q}, n_q,\theta_0^q,\theta_n^q) \frac{e^{-jk\rho_q}}{\sqrt{\rho_q}} \qquad (3)$$

The surface wave is added for the multiple diffractions between edges, because it is for these terms that a surface wave would be expected to

propagate along the face from one diffracting edge to the next.

III. ANALYTICAL RESULTS

In all of the cases considered in this paper, the dihedral corner reflector is assumed to be constructed of two square plates measuring 5.6088λ on each side, and a frequency of 9.4 GHz was considered. The calculations are made in the principle plane and the radar cross section area is presented in decibels relative to a square meter (dBsm). The region near the bisector (ϕ=0) of the included angle of the dihedral is referred to as the forward region. The typical dihedral corner reflector backscatter pattern is characterized by large specular lobes at normal incidence to any of the flat plate surfaces. In addition, the right angled corner has a strong specular double reflection which gives a large cross section in the forward region. However these expected specular lobes can be signicantly altered by appropriate choices of the surface impedances.

The first computed cross section patterns considered compare the UTD theory for lossy surfaces developed in this work with a moment method (MM) technique [15] for verification of the accuracy of the UTD solution. The moment method technique is based on a surface-patch model of a dipole sinusoidal surface current mode [15]-[16]. The impedance boundary condition utilized in the moment method solution is appropriate for perfectly conducting sheets coated with lossy materials [17]-[18]. The lossy coating material selected is a narrow band dielectric/ferrite absorber with ε_r=7.8-j1.6 and μ_r=1.5-j0.7 with coating thickness of

$t=0.065\ \lambda$ [18]. This material coating corresponds to a normalized surface impedance of $\eta=0.453-j0.053$.

In Fig. 2, the 90° dihedral corner reflector is examined in the full azimuthal plane for both coated and uncoated conducting plates for the vertical polarization. The uniform geometrical theory of diffraction developed in this work is compared to the moment method technique of [15] in this figure. The 90° corner reflector is characterized by a dominant double reflected field in the forward region and large specular lobes at the four observation directions which are normal to each of the four surfaces. The lossy surface coating reduces the cross section of the corner reflector substantially. The specular single reflections are reduced by about 8.6 dB while the double reflection is reduced by 12 dB due to the fact that the loss is incurred at each reflection. The loss is not doubled because the incidence angle is different for the double reflection than for the single reflection.

In Fig. 3, corresponding patterns for the 98° corner reflector are examined. Again UTD and MM are compared for both coated and uncoated corner reflectors. The cross section pattern is consistently lowered by 8 to 10 dB in most regions by application of the surface coating. It is also evident that by utilizing an angle other than 90° the dominant double reflection term is removed. Hence it is important to consider both the geometry and the material composition for optimum cross section reduction.

In Fig. 4, the 77° corner reflector is considered. The acute angle also removes the strong specular double reflection although not

as effectively as the obtuse angled corner. For this reflector the higher order scattering components play a more significant role in determining the total cross section. The acute angled reflector also shows the largest differences between the UTD and MM techniques in the forward region due to the many higher order mechanisms occurring.

Of particular interest in reducing the specular lobes are those surface impedances for which the surface is matched to the free space value. At a particular angle of incidence φ, measured from the face of the wedge, the normalized surface impedance η can be selected to appear as a match to the incident wave by choosing

$$\eta = \frac{1}{\sin\varphi} \qquad \text{for the soft (vertical) polarization} \qquad (4a)$$

$$\eta = \sin\varphi \qquad \text{for the hard (horizontal) polarization} \qquad (4b)$$

These surface impedances provide a match for a plane wave on a planar boundary, but only approximate a match for the finite plates of the corner reflector. It is recognized that these surface impedance are often very difficult to achieve using physical materials; however they are interesting because they provide an upper limit on the cross section reduction using uniform surface impedances. Better reductions may be achieved using tapered surface impedances.

The cross section patterns displayed in Fig. 5 are for a 90° dihedral corner reflector illuminated by a vertically polarized wave. In this figure, the pattern of the perfectly conducting reflector is compared with patterns of a variety of lossy surface impedances. The perfectly conducting cross section has large specular lobes at $\phi = \pm 45^\circ$ and the large double reflection in the forward region. Introducing a

small loss, corresponding to η=0.2, reduces the cross section pattern nearly everywhere and effectively lowers the double reflection contribution more than the single reflection because the loss is encountered once at each reflection. To achieve maximum reduction of the specular single reflection, the surface impedance must match the free space value; hence a normalized surface impedance of η=1.0 must be selected. It is noted that this choice of normalized surface impedance effectively annihilates the single specular reflection but cannot remove the double reflection term for which the incident wave makes an angle of approximately 45° with the reflecting plates. Selecting $\eta=1/\sin(45^\circ)=1.414$ effectively eliminates the large double reflected field but cannot remove the single reflections. To achieve better results, it may be profitable to attempt tapered surface impedances.

The horizontal polarization patterns for the same dihedral corner reflector are displayed in Fig. 6. The patterns for the perfectly conducting (η=0) and the lossy (η=0.2) surfaces show a similar lobe structure as noted for the vertical polarization, and the cross section reduction with increasing loss is considered. The perfectly matched single reflection case, η=1.0, is mathematically identical to the vertical polarization, and it is not shown. They are identical because the symmetries of Maxwell's equations and the impedance boundary condition stipulate that a change in polarization is equivalent to using the reciprocal of the normalized surface impedance. Similarly the η=0.707 pattern displayed in Fig. 6 for the horizontal polarization is identical to the one for η=1.414 displayed in Fig. 5 for the vertical polarization. These surface impedances are selected because they

provide the maximum reduction of the double reflected field for the associated polarization. However it is also of interest to investigate the cross section pattern when a target is designed for one polarization yet illuminated by the other polarization. In Fig. 6 the case η=1.414, which successfully reduced the vertically polarized double reflection in Fig. 5, does not perform well under horizontal illumination. By symmetry, this pattern also corresponds to η=0.707 for the vertical polarization, and therefore also illustrates the degradation for a reflector designed for horizontal polarization but illuminated by vertical polarized waves.

To achieve a useful reduction in the cross section over the entire azimuthal plane, it is often necessary to utilize different impedances over different surfaces. In Fig. 7, patterns in both the forward and back regions of 90° corner reflector with various surface impedances are displayed for horizontal polarization. As expected, the perfectly conducting case has the strongest response. The small loss, η=0.2, effectively reduces the cross section pattern in most regions. To achieve maximum reduction of the back lobes, surfaces 6 and 8 must both be loaded with normalized impedances of η=1.0. In the forward region, η=1.0 would reduce the single reflection at the expense of the double reflection, while η=0.707 would reduce the double reflection at the expense of the single reflection. By iterative methods it was determined that an intermediate value of η=0.92 for surfaces 2 and 4 yielded the lowest maximum of the radar cross section pattern in the forward region. The cross section pattern of this lossy corner reflector, with a different impedance on the front than on the back, is

as shown in Fig. 7. The maximum lobe was reduced from 15.6 dBsm to -16.8 dBsm, an effective reduction of 32.4 dB.

IV. CONCLUSIONS

The corner reflector is a very important geometry to study because it demonstrates many of the scattering properties of more complex targets. Hence it is possible to infer the scattering characteristics of other geometries from the characteristics of the corner reflector. The UTD is especially useful for this purpose because it isolates individual scattering mechanisms, and, in contrast to the moment method, it allows the dominant terms to be identified. In this work it was shown that the UTD is also accurate in that it compares well with moment method techniques for coated corner reflectors which may have right, acute, or obtuse interior angles.

To achieve good cross section reduction, it was demonstrated that one must select an appropriate wedge angle as well as a good surface coating material. For more complicated geometries, this implies that the specular reflections should be eliminated when possible, especially by avoiding right angled corners. Obtuse angles are preferred because they divert the strong double reflected wave away from the backscatter direction without inducing more multiple reflections. Acute corners develop larger multiple reflections and diffractions which tend to make the cross section reduction more difficult to achieve. By choosing an appropriate wedge angle it is often possible to achieve a null in the forward region rather than a maximum as was illustrated for the 98°

corner reflector considered here.

To effectively use surface impedance coatings requires that the dominant scattering terms be identified, and the UTD is well suited for this purpose. Surface impedances should be selected which match the dominant terms as closely as possible in regard to their individual incidence angles. In practice however, it may not always be possible to fabricate layered coatings to meet the optimum requirements especially with practical thickness or weight constraints. It was demonstrated in this work that lossy coatings should be utilized differently for interior corners than for exterior corners because for the interior faces the higher order reflections and diffractions are often the dominant terms, and each may have a different angle of incidence. It was also established that a design for one polarization may not be effective for another polarization. As illustrated for the corner reflector, if the double reflection is eliminated for one polarization, it may still prevail for the other polarization. Practically, one might propose using polarization-sensitive material compositions which present different impedances to the two primary polarizations. In addition, it was shown that reduction in one scattering component can usually be achieved only at the expense of some other component, as was demonstrated for the single and double reflected terms in the corner reflector analysis. Tradeoffs in the selected impedance values must often be considered to achieve optimum results. The use of tapered impedances can help to alleviate this situation; however the UTD method utilized here cannot consider tapered impedances due to the exact solution upon which it is based.

V. PUBLICATIONS

During this reporting period two papers have been submitted for publication in IEEE refereed papers and three papers were presented in international symposia. The work reported in all of these papers was supported by this NASA Grant. These are as follows:

a. T. Griesser, C. A. Balanis and K. Liu, "Analysis and reduction for lossy dihedral corner reflectors," submitted for publication in Proc. IEEE.

b. T. Griesser and C. A. Balanis, "Reflections, diffractions, and surface waves for an interior impedance wedge of arbitrary angle," submitted for publication in IEEE Trans. Antennas Propagation.

c. L. A. Polka, C. A. Balanis and K. Liu, "Comparison of higher-order diffractions in scattering by a strip," 1988 IEEE AP-S International Symposium, June 6-10, 1988, Syracuse, NY.

d. T. Griesser and C. A. Balanis, "Reflections, diffractions, and surface waves for an interior wedge with impedance surfaces," 1988 IEEE AP-S International Symposium, June 6-10, 1988, Syracuse, NY.

e. T. Griesser and C. A. Balanis, "Calculation of the Fresnel transition function of complex argument for the method of steepest descents," 1988 URSI Radio Science Meeting, June 6-10, 1988, Syracuse, NY.

VI. FUTURE WORK

Future work on this project will concentrate on applying reflection, diffraction and surface waves from wedges (interior and exterior) with impedance surface to predict the patterns from lossy surfaces. This is to include surfaces with discontinuities as well as other complex targets. In addition equivalent concepts will be examined to predict the scattering patterns of perfectly conducting and lossy surfaces along principal and nonprincipal planes.

REFERENCES

[1] T. Griesser and C. A. Balanis, "A uniform geometrical theory of diffraction for an interior impedance wedge with surface waves," submitted for publication.

[2] R. Tiberio, G. Pelosi, and G. Manara, "A uniform GTD formulation for the diffraction by a wedge with impedance faces," *IEEE Trans. Antennas Propagat.*, vol. AP-33, no. 8, pp. 867-873, Aug. 1985.

[3] M. I. Herman and J. L. Volakis, "High frequency scattering from canonical impedance structures," University of Michigan Radiation Laboratory Technical Report 389271-T, Ann Arbor, Michigan, May 1987.

[4] N. G. Alexopoulos and G. A. Tadler, "Accuracy of the Leontovich boundary condition for continuous and discontinuous surface impedances," *Journal of Applied Physics*, vol. 46, no. 8, pp. 3326-3332, Aug. 1975.

[5] D. Wong, "Limits and validity of the impedance boundary condition on penetrable surfaces," *IEEE Trans. Antennas Propagat.*, vol. AP-35, no. 4, pp. 453-457, April 1987.

[6] S. W. Lee and W. Gee, "How good is the impedance boundary condition?," *IEEE Trans. Antennas Propagat.*, vol. AP-35, no. 11, pp. 1313-1315, Nov. 1987.

[7] E. F. Knott, "RCS reduction of dihedral corner reflectors," *IEEE Trans. Antennas Propagat.*, vol. AP-25, no. 3, pp. 406-409, May 1977.

[8] W. C. Anderson, "Consequences of nonorthogonality on the scattering properties of dihedral reflectors," *IEEE Trans. Antennas Propagat.*, vol. AP-35, no. 10, pp. 1154-1159, October 1987.

[9] T. Griesser and C. A. Balanis, "Backscatter analysis of dihedral corner reflectors using physical optics and the physical theory of diffraction," *IEEE Trans. Antennas Propagat.*, vol. AP-35, no. 10, pp. 1137-1147, October 1987.

[10] A. Michaeli, "A closed form physical theory of diffraction solution for electromagnetic scattering by strips and 90° dihedrals," *Radio Science*, vol. 19, no. 2, pp. 609-616, March-April 1984.

[11] C. L. Yu and J. Huang, "Air target analytical model," Naval Weapons Center, China Lake, CA, Int. Rep.

[12] T. Griesser and C. A. Balanis, "Dihedral corner reflector backscatter using higher order reflections and diffractions," *IEEE Trans. Antennas Propagat.*, vol. AP-35, no. 11, pp. 1235-1247, Nov. 1987.

[13] P. Corona, G. Ferrara, and C. Gennarelli, "Backscattering by loaded and unloaded dihedral corners," *IEEE Trans. Antennas Propagat.*, vol. AP-35, no. 10, pp. 1148-1153, October 1987.

[14] T. Griesser, "High-frequency electromagnetic scattering from imperfectly conducting structures," Ph.D. Dissertation, Arizona State Univ., Tempe, June 1988.

[15] K. Liu, C. A. Balanis and T. Griesser, "A dipole surface-patch current mode for large body three-dimensional scattering problems," to be published.

[16] J. H. Richmond, D. M. Pozar, and E. H. Newman, "Rigorous near-zone field expressions for rectangular sinusoidal surface monopole," *IEEE Trans. Antennas Propagat.*, vol. AP-26, no. 3, pp. 509-510, May 1978.

[17] K. M. Mitzner, "Effective boundary conditions for reflection and transmission by an absorbing shell of arbitrary shape," *IEEE Trans. Antennas Propagat.*, vol. AP-16, no. 6, pp. 706-712, Nov. 1968.

[18] E. H. Newman and M. R. Schrote, "An open surface integral formulation for electromagnetic scattering by material plates," *IEEE Trans. Antennas Propagat.*, vol. AP-32, no. 7, July 1984.

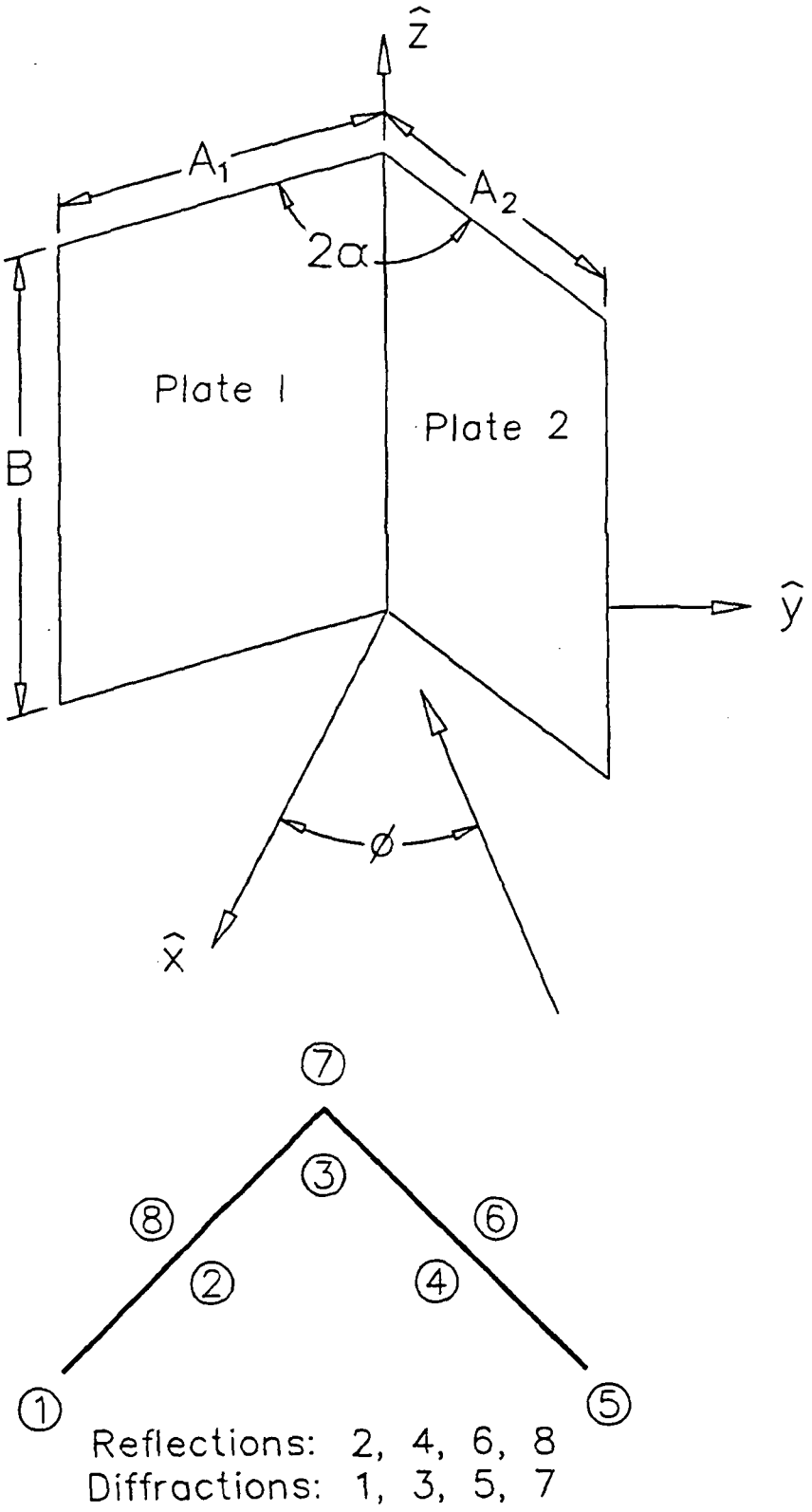

Fig 1. The dihedral corner reflector geometry and numbering convention.

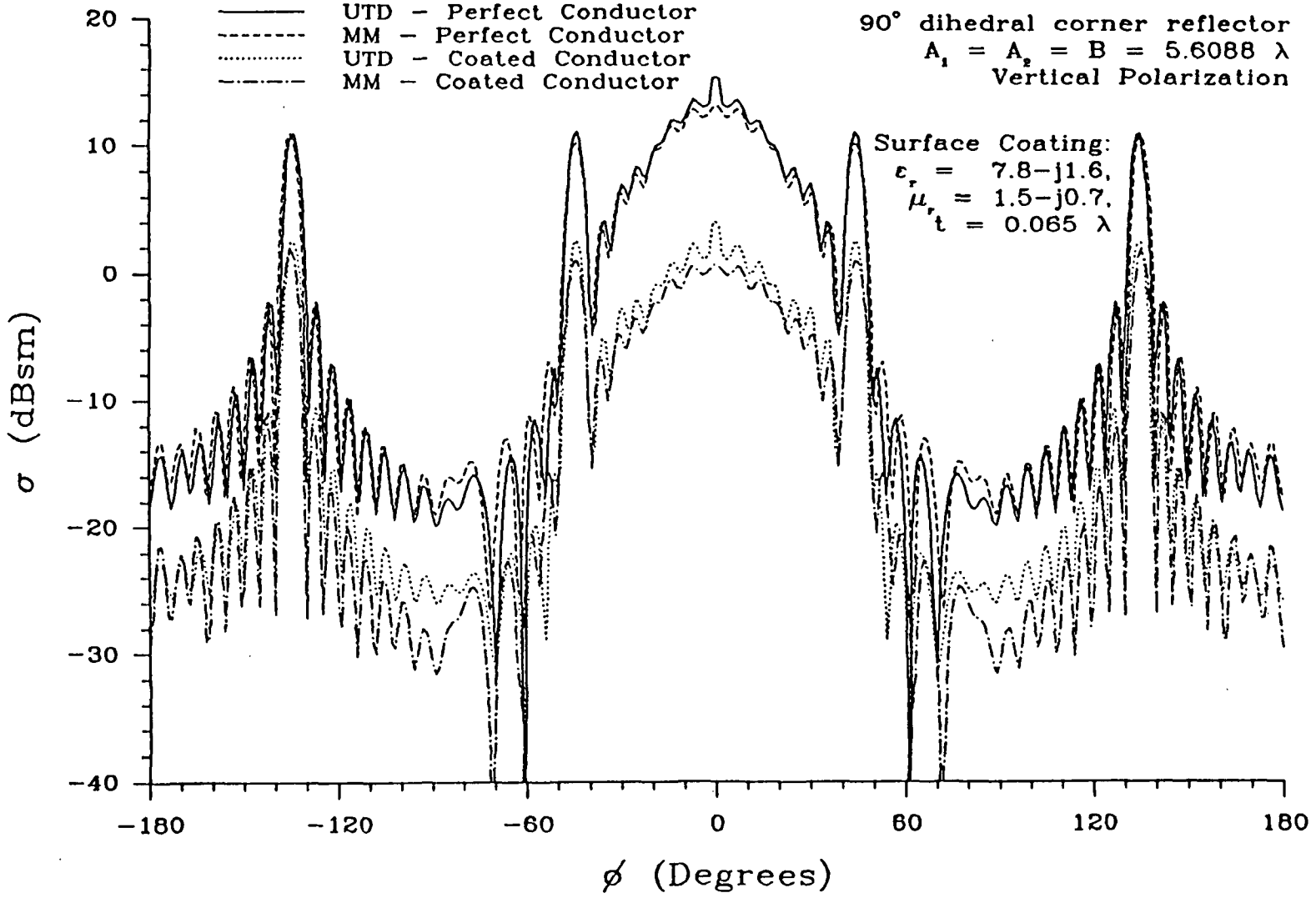

Fig. 2. Comparisons of UTD and MM for 90° perfectly conducting and coated reflectors.

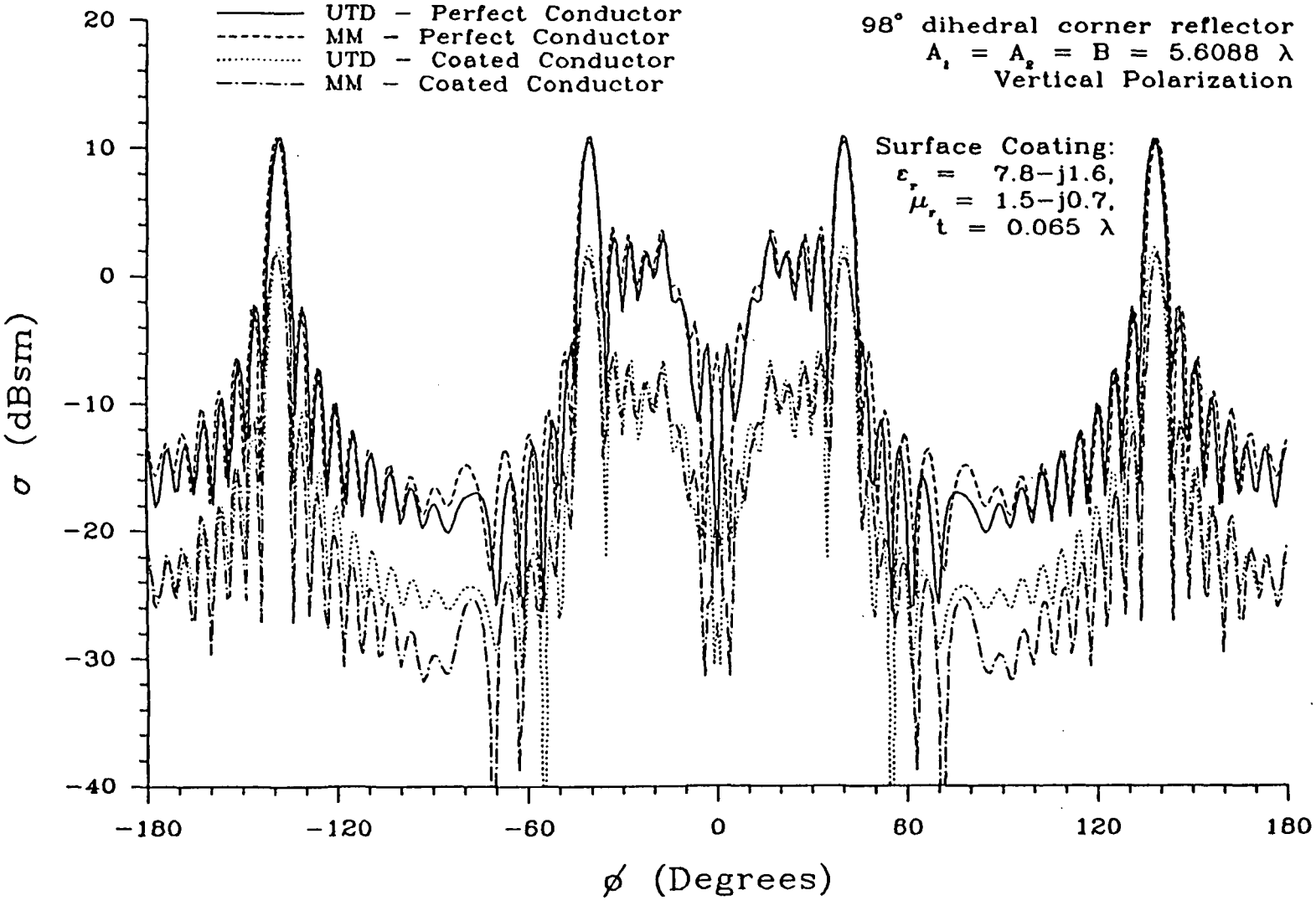

Fig. 3. Comparisons of UTD and MM for 98° perfectly conducting and coated reflectors.

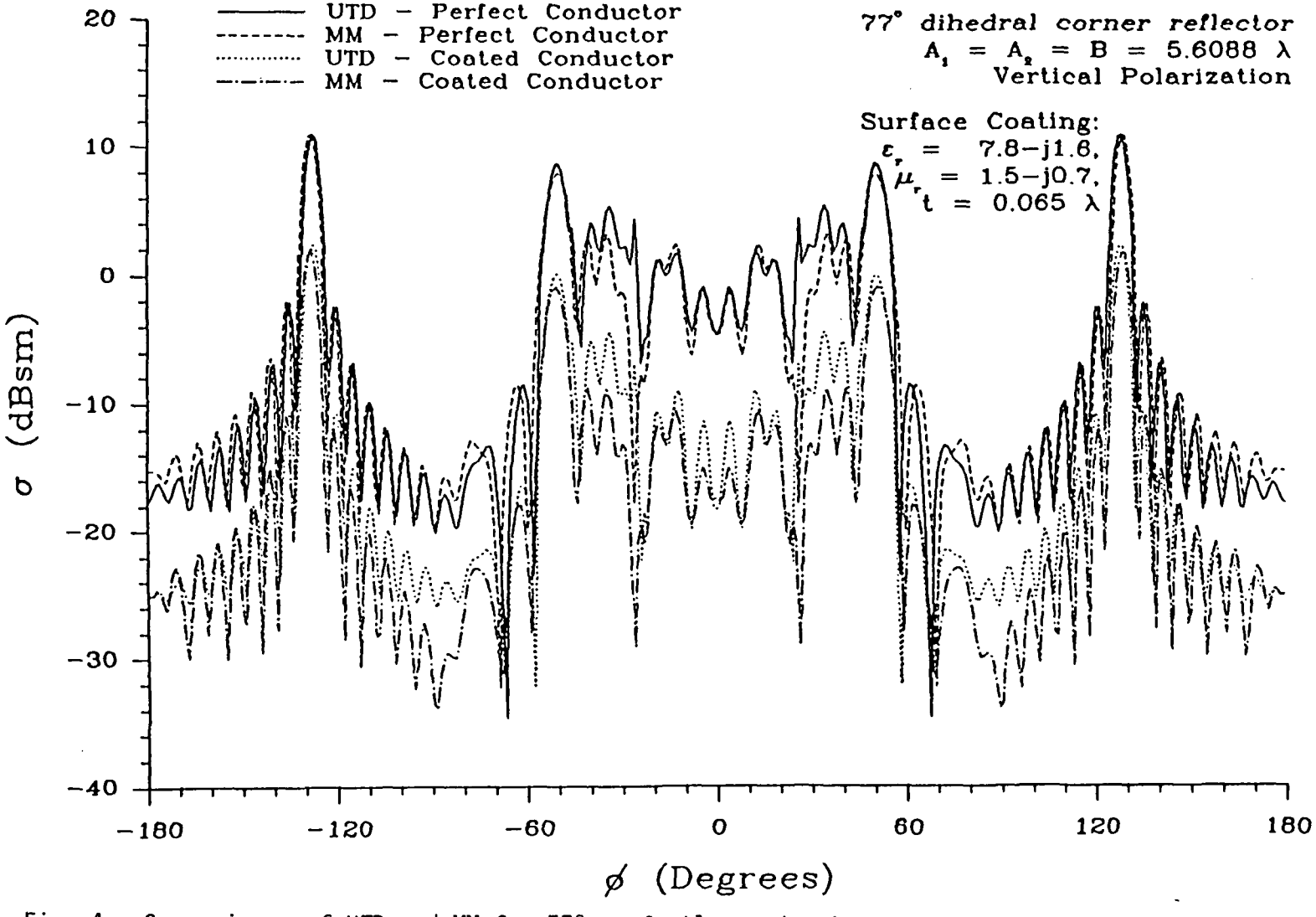

Fig. 4. Comparisons of UTD and MM for 77° perfectly conducting and coated reflectors.

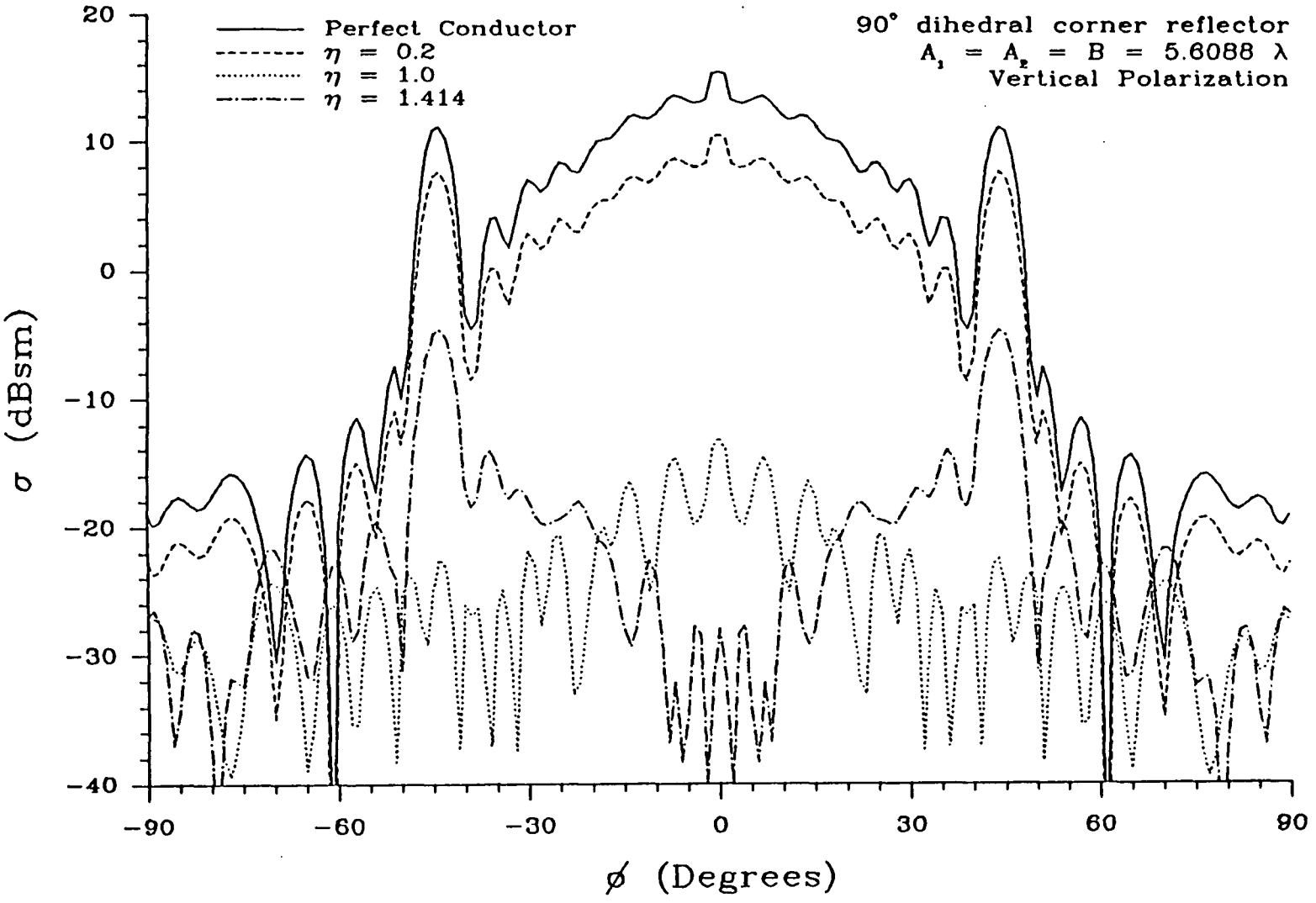

Fig. 5. Reduction of the 90° reflector cross section for vertical polarization.

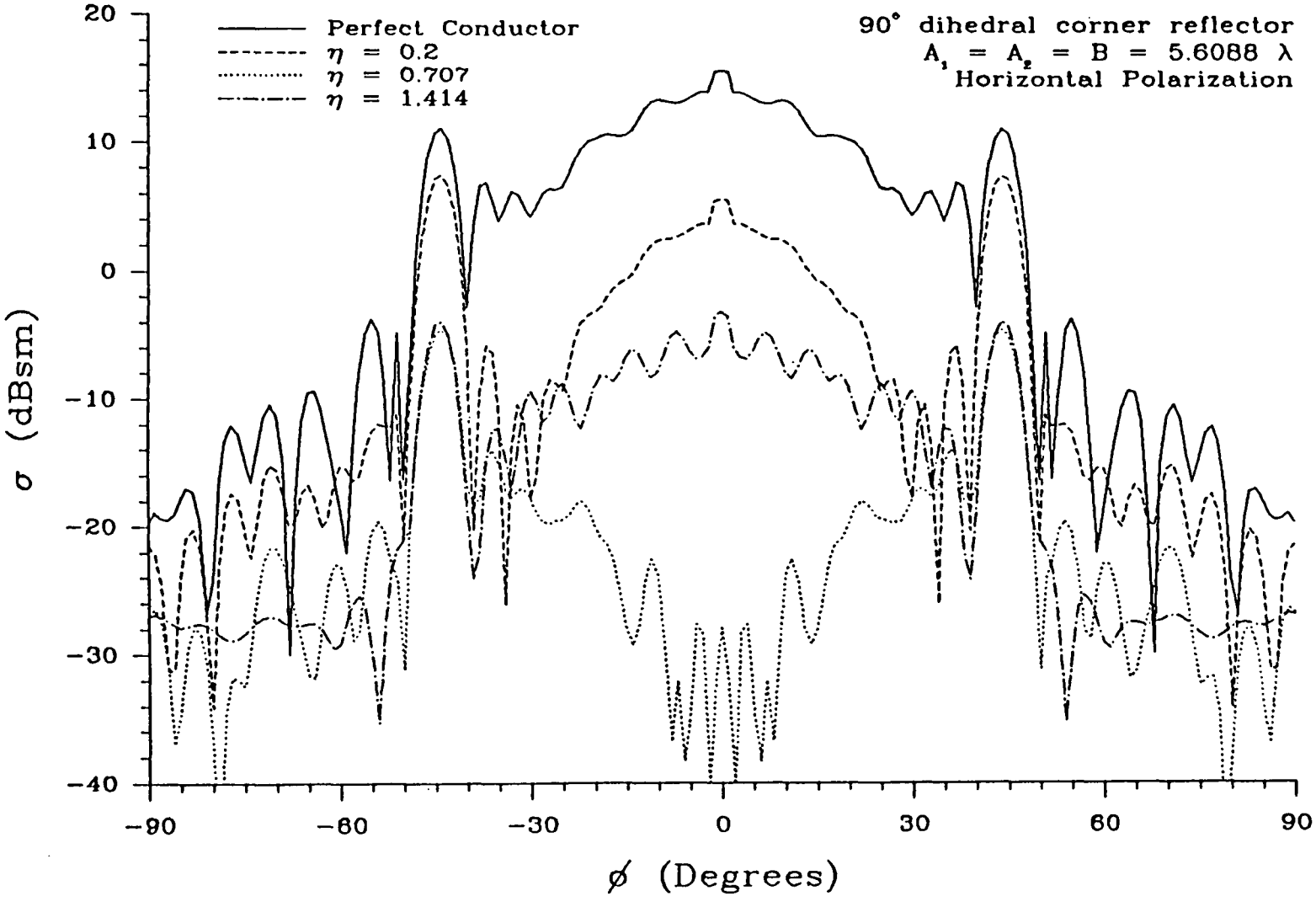

Fig. 6. Reduction of the 90° reflector cross section for horizontal polarization.

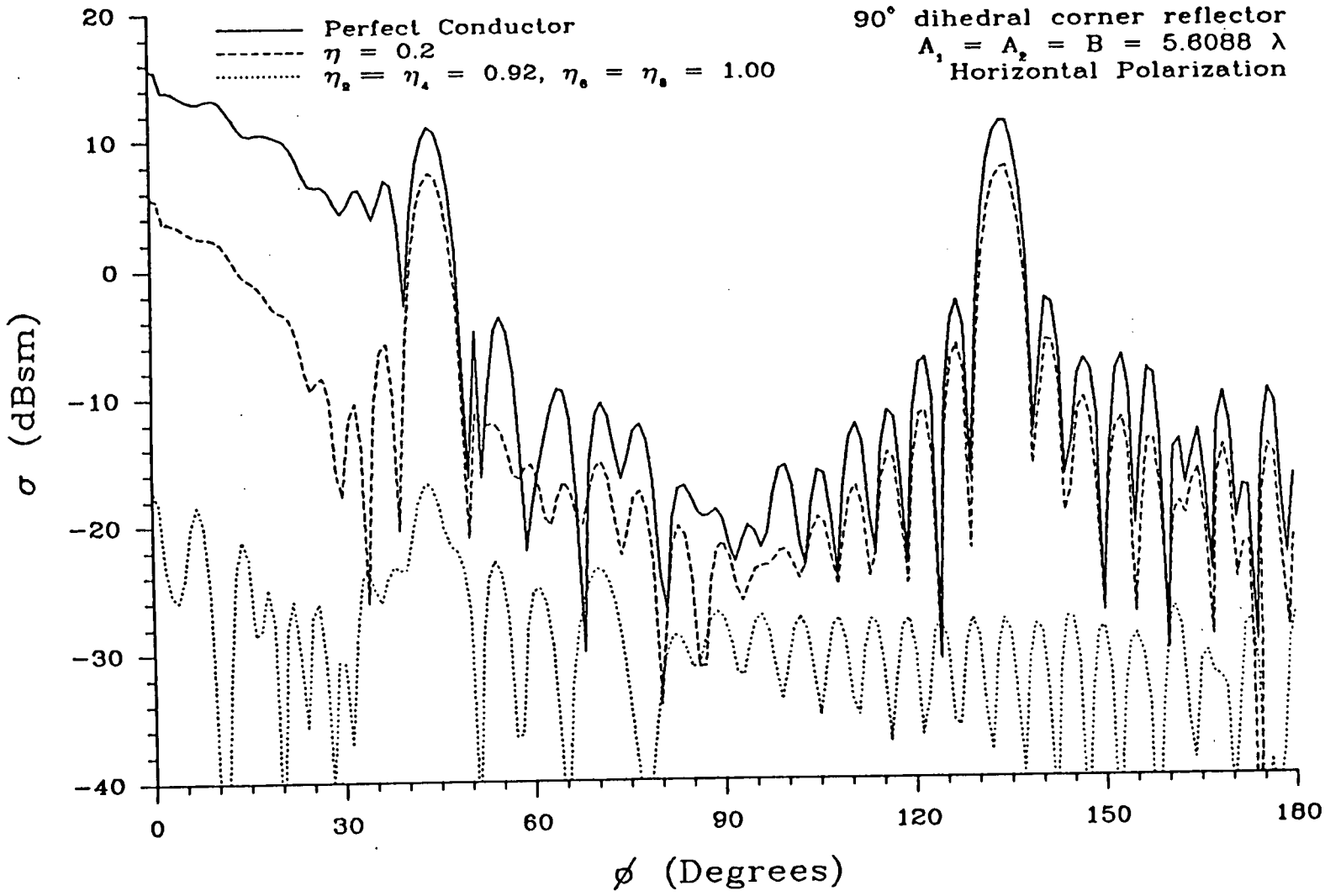

Fig. 7. Reduction of specular lobes in the forward and back regions for the 90° reflector.